



Cr, Zr-incorporated hydrotalcites and their application in the synthesis of isophorone

Yanxia Liu^{a,b}, Kunpeng Sun^a, Haowen Ma^c, Xianlun Xu^{a,*}, Xiaolai Wang^{a,*}

^a State Key Laboratory for Oxo Synthesis and Selective Oxidation, Lanzhou Institute of Chemical Physics, Chinese Academy of Sciences, Lanzhou 730000, China

^b Graduate University of Chinese Academy of Sciences, Beijing 100039, China

^c Lanzhou Petrochemical Research Center of Petrochina, Lanzhou 730000, China

ARTICLE INFO

Article history:

Received 6 January 2010

Received in revised form 16 March 2010

Accepted 26 March 2010

Available online 1 April 2010

Keywords:

Cation-incorporated hydrotalcite

Condensation

Isophorone

Solid base

ABSTRACT

Cr³⁺ and Zr⁴⁺ cation-incorporated hydrotalcites (HTs) were prepared by coprecipitation method. Corresponding mixed oxide were obtained by the thermal decomposition of HTs at 773 K for 8 h and applied in the synthesis of isophorone (IP) from acetone. From the characteristic results, both Cr³⁺ and Zr⁴⁺ were introduced into the lattice of hydrotalcite producing the more disordered HT structures. Compared with Mg–Al mixed oxide, Cr and Zr modified mixed oxide demonstrated more amount of basic sites and stronger base strength, which were responsible for the improvement of catalytic activity. As a result, both of the modified mixed oxide exhibited IP selectivity of more than 70% under atmospheric pressure.

© 2010 Elsevier B.V. All rights reserved.

1. Introduction

Hydrotalcite (HT) or layered double hydroxide (LDH), e.g. Mg₄Al₂(OH)₁₂CO₃·4H₂O, has a structure similar to that of brucite, Mg(OH)₂ [1]. In brucite, Mg²⁺ are octahedrally coordinated by hydroxyl ions, which are edge-shared to form a sheet-like structure. In HT, some of Mg²⁺ are replaced by Al³⁺, resulting in a net positive charge of the brucite-like layers. Charge-balancing anions (typically CO₃²⁻) and water molecules are situated in the interlayers between the stacked brucite-like cation layers [2]. Upon calcinations, the dehydroxylation of layers and the decomposition of carbonates take place, leading to formation of a mixed oxide phase, Mg(Al)O. The mixed oxide holds both strong Lewis basic and mild Lewis acid sites. The former are due to the presence of the oxygen atoms of low coordination, and the latter to Al³⁺ cations [3]. The acid-base properties of the mixed oxide are related to its composition, preparation method, and treatment conditions (calcination temperature) [4]. In HT, Mg²⁺ and Al³⁺ can be partially substituted by other metal ions, which often introduced new catalytic properties [5,6]. The cation-incorporation is also an efficient method of modifying the acid-base property of the mixed oxide.

Isophorone (IP) is a kind of excellent high boiling solvent and important chemical intermediate. It was typically synthesized from acetone. As shown in Fig. 1, acetone firstly condensed and dehydrated to produce mesityl oxide (MO) or isomesityl oxide (IMO), then the MO condensed with another molecular of acetone and IP was formed via 1,6-Michael addition [7] or 1,6-Adol condensation reaction [8]. All

these reactions mentioned above can be catalyzed by solid base [9]. Mg–Al mixed oxide derived from hydrotalcite has been applied in the synthesis of IP in many previous studies [10–13]. A. A. Schutz prepared hydrotalcite like material by suspending alumina gel and MgO. The derived Mg–Al mixed oxide exhibited high selectivity of IP (74.5%) under 623 K and 15 PSIG [10]. Because the complexity of the preparing method, new preparing methods were continuously reported [11–13]. Recently, Wang and coworkers [13] prepared HT through coprecipitation-constant-temperature-crystal method and the derived Mg–Al mixed oxide exhibited acetone conversion of 17.7% and IP selectivity of 65.3% under 523 K. These reports mainly studies on the method of synthesis hydrotalcite-like material, which was precursor of the Mg–Al mixed oxide. But limited literatures is available on the cation-doped Mg–Al mixed oxide for the synthesis of IP. In this work, HTs incorporated by Cr and Zr were synthesized through coprecipitation method and the Cr and Zr doped Mg–Al mixed oxides were applied in the synthesis of IP. Results showed that the doped mixed oxides exhibited excellent catalytic performance and should be potentially used in the synthesis of IP.

2. Experimental

2.1. Catalyst preparation

The mixed nitrates (Mg:Cr/Zr:Al=39:1:20) with appropriate molar ratio were dissolved in distilled water. Another aqueous solution containing NaOH and Na₂CO₃ (molar ratio of NaOH and Na₂CO₃=4:1) was added to the above solution at 353 K under stirring. The mixture was stirred at the same temperature for 5 h. Then the precipitate was filtered, washed and dried at 393 K for 12 h.

* Corresponding authors. Tel./fax: +86 931 4968217.

E-mail addresses: mibkcat@gmail.com (X. Xu), mibkcat@gmail.com (X. Wang).

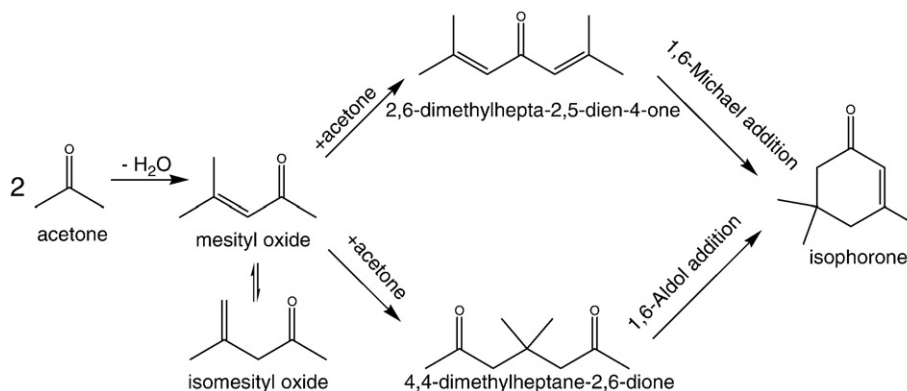


Fig. 1. General reaction mechanism for synthesis of isophorone.

The as-synthesized hydrotalcite was denoted as M/HTas in which M represented the modified metal cations. In the same fashion, the sample calcinated at 773 K for 8 h was denoted as M/HTox. For comparison, the hydrotalcite HTas with molar ratio of Mg/Al = 2:1 and the corresponding mixed oxide HTox were prepared via the same method.

2.2. Catalyst characterizations

X-ray diffraction (XRD) patterns were obtained by Philips X Pert Pro X diffractometer operated with a Ni-filtered Cu K α radiation. Physisorption of N₂ was carried out at 77 K on a volumetric apparatus (ASAP 2020). Temperature-programmed desorption of CO₂ (CO₂-TPD) was performed on a homemade instrument. Typically, 50 mg of sample was firstly pretreated in helium at 823 K for 30 min, then the temperature was cooled to 323 K and the sample was saturated with CO₂. Desorption of CO₂ was carried out from 323 K to 823 K under flowing helium (30 mL/min) using a temperature rate of 10 K/min.

2.3. Catalytic activity test

The reactions were carried out in a fixed-bed microreactor (6 mm i.d.) using 0.6 g of catalyst under atmospheric pressure. Acetone and N₂ were fed into the reactor from the top and mixed in preheating section. The N₂ (20 mL/min) was introduced with two aims. Firstly, N₂ flow can avoid the interaction between catalyst and CO₂ in air. Secondly, it can carry away the product timely and prevent the further-condensations. The experiments were carried out at 513 K for 2 h. The products were collected in a cold trap (held in an ethanol/dry ice bath) and quantified by gas-chromatography (GC) equipped with a flame ionization detector (FID).

3. Results and discussion

3.1. Characterizations

The lattice parameters and particle sizes of the hydrotalcites are shown in Table 1. The lattice parameters *a* and *c* were calculated from the expression $a = 2d_{(110)}$ and $c = 3d_{(003)}$, respectively. The average particle sizes in the *a*- and *c*- directions were determined from full

width at half maximum (FWHM) of (110) and (003) diffraction peaks, using the Debye-Scherrer formula. The parameters *a* and *c* of Cr/HTas and Zr/HTas were bigger than that of HTas. The enlargement of *a* of Zr/HTas was related to the replacement of Mg²⁺ (0.65 Å) or Al³⁺ (0.50 Å) by cations with larger ionic radius Zr⁴⁺ (0.72 Å). As is known, The radius of Zr⁴⁺ is larger than that of Cr³⁺ (0.62 Å). However, the enlargement of *a* of Cr/HTas was larger than that of Zr/HTas. This may be indicative of less introduced Zr⁴⁺ due to its larger radius. The parameter *c* also showed the same tendency of *a*, which can be attributed to the increase of the thickness of the brucite-like layer upon incorporation of Cr³⁺ or Zr⁴⁺ [14]. The dimension of HTas in *a*-direction was larger than that in *c*-direction, which was typical for the plate-like hydrotalcite crystals [15]. Compared with HTas, particle size of Cr/HTas and Zr/HTas was smaller. Moreover, their particle sizes in *a*-direction was smaller than those in *c*-direction, indicating formation of more irregular structures.

The XRD patterns of the as-prepared hydrotalcites were shown in Fig. 2 A. All the three patterns showed the characteristic diffraction lines typical for an HT compound, proving the formation of hydrotalcite-like structure. There were no other diffraction peaks observed on patterns of Cr/HTas and Zr/HTas, indicating that the modified cations were incorporated into the lattice or highly dispersed on the surface. Combined with the enlargement of lattice parameter *a* of the Cr/HTas and Zr/HTas, the incorporations of the modified cations were confirmed. After heat treatment of HTas at 773 K the layered compound was destroyed and the mixed oxide (Mg(Al)O) was formed. From the XRD patterns of the calcined mixed oxide (Fig. 2 B), Cr/HTox displayed pattern similar to that of HTox. Besides diffraction peaks corresponding to the Mg(Al)O, there was another diffraction peak around 30° shown in pattern of Zr/HTox. This peak could be attributed to ZrO₂ (88-1007), which suggested that the incorporation of large atom Zr was not stable in the calcination process. Upon calcinations, color of Cr-modified hydrotalcite changed from grey-blue of Cr/HTas to yellow of Cr/HTox. The former was typically displayed by Cr (III) and the latter by Cr (VI). These phenomena implied that both the coordination number and valence of Cr changed in calcination process.

The texture properties of the mixed oxides were shown in Table 2. Compared with those of HTox, the surface area, pore volume and pore size of Cr/HTox slightly decreased. These results could be indicative of the similar structure of these two samples. Zr/HTox showed remarked different texture properties, which implied significant modifications stemming from the incorporation of Zr. Larger pore size of Zr/HTox deduced the smaller surface area and pore volume. It was reported that there was more interlayer waters in the Zr-modified hydrotalcite [14]. This larger pores may be related to the departure of more water molecules.

CO₂-TPD was usually employed to determine the density and strength of basic sites in mixed oxides derived from the hydrotalcites. The CO₂ as probe molecule has enough acidity to probe all the basic

Table 1
Parameters from the XRD.

Sample	Cell parameter (Å)		Particle size (Å)	
	<i>a</i>	<i>c</i>	<i>d</i> (110)	<i>d</i> (003)
HTas	3.045	22.765	1421.5	557.0
Cr/HTas	3.048	22.887	409.3	424.6
Zr/HTas	3.046	22.842	314.6	466.3

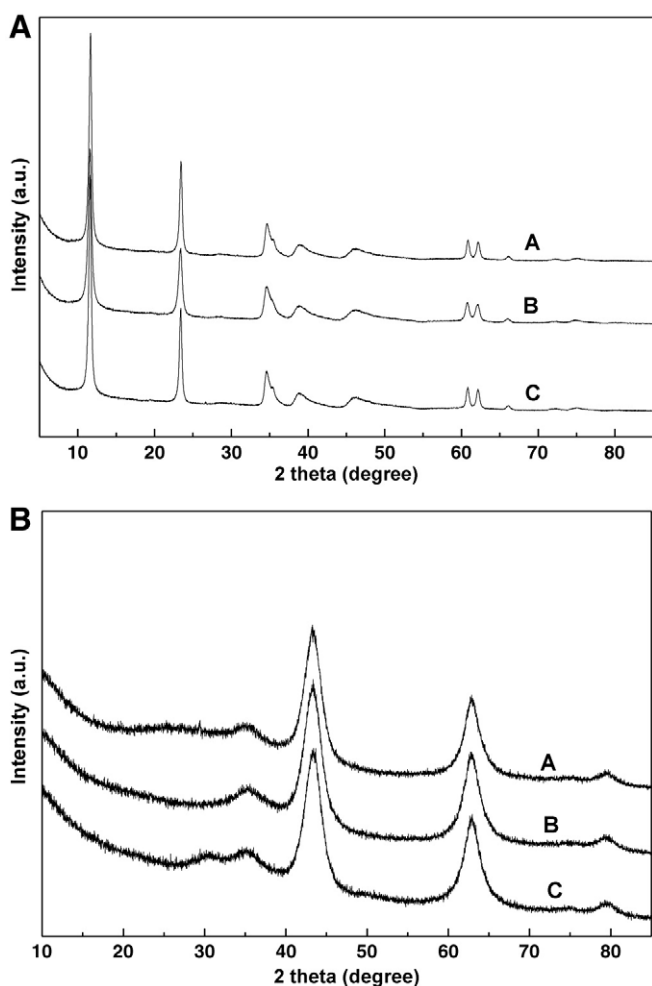


Fig. 2. XRD patterns of M/HTas (a) and M/HTox (b): A. HT, B. Cr/HT and C. Zr/HT.

sites [16]. CO₂-TPD curves of the calcinated samples were shown in Fig. 3. The desorption of CO₂ from HTox started as low as 350 K reaching the maximum at about 400 K. Moreover, a shoulder centered at about 550 K was observed in the recorded desorption profiles. CO₂-TPD curves of Cr/HTox and Zr/HTox showed two desorption peaks, indicating the existence of at least two types of basic sites. It is reported that the low-temperature maximum of CO₂ desorption centered at about 400 K was attributed to carbon dioxide species adsorbed on weakly basic OH groups [17] and the high-temperature CO₂ desorption peak observed at 550 K was assigned to CO₂ adsorbed on O²⁻ anions [18]. The stronger basic strength of Zr/HTox may be related to the higher net electronic charge of the layers in Zr/HTas, which resulted in more low coordination oxygen atoms. The high-temperature peak of Cr/HTox was found between 550 K and 800 K. The shift of the desorption peak of Cr/HTox to higher temperature may be caused by the higher value of electronegativity of Cr than that of Mg and Al.

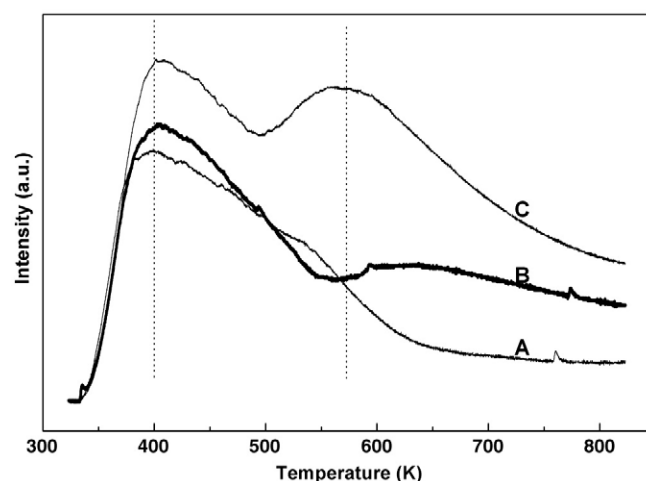


Fig. 3. CO₂-TPD curves of calcined hydrotalcite: A. HTox, B. Cr/HTox and C. Zr/HTox.

3.2. Synthesis of IP

Acetone aldol condensation were tested at 513 K under atmospheric pressure. The obtained results over different catalysts are shown in Table 3. The main products detected were MO, IMO, IP, 2,6-dimethylhepta-2,5-dien-4-one (also denoted as phorone), 4,4-dimethylheptane-2,6-dione and minor quantities of further-condensation products. From Table 3, the modified mixed oxide exhibited improved catalytic performance compared with result of HTox. This improvement of catalytic activity was consistent with the results of CO₂-TPD. From results of the CO₂-TPD, Cr/HTox and Zr/HTox showed stronger basic strength and larger amount of the basic site than HTox, expressed by the corresponding temperature and area of peaks. The Zr/HTox showed the biggest area of the desorption peaks. Accordingly, Zr/HTox exhibited the highest acetone conversion of 36.8%. Furthermore, more irregular structure of the modified hydrotalcite were also beneficial for the increased catalytic activity. It was reported that only basic sites near edges of hydrotalcite platelets took part in aldol condensations [2]. More active basic sites were available in the irregular modified mixed oxide leading to higher acetone conversions over the modified mixed oxide. According to the reference [19], the selectivity of IP depends on the strength of the basic site. The acetone oligomerization can only be achieved over strong basic sites. The presence of more strong basic sites on Zr/HTox and Cr/HTox was helpful to the high selectivity of IP. MO or IP cannot desorb from the stronger basic site timely which make further condensations take place. As a result, there are more further condensed by-products besides IP detected from the GC results of Cr/HTox and Zr/HTox.

The time-on-stream behavior for acetone condensation on Cr/HTox was tested and shown in Fig. 4. A progressive deactivation process was observed in 12 h. During the catalyst decay, formation of MO increases at expense of IP. Similar result has been observed by J.I. Di Cosimo et al. on Mg–Al mixed oxide derived by HT synthesized by coprecipitation method [20]. Because the main reason of the deactivation was coke formation caused by Adol condensation synthesis of tetramers and

Table 2
Texture properties of the materials.

Sample	S _{BET} ^a (m ² /g)	V _{pore} ^b (cm ³ /g)	Pore size ^c (nm)
HTox	147.0	0.9137	21.5
Cr/HTox	137.3	0.7458	19.4
Zr/HTox	105.8	0.4449	24.1

^a BET surface area.

^b Single point total volume at P/P₀ = 0.97.

^c BJH desorption average pore diameter.

Table 3
Activity result of acetone condensation^a.

Catalyst	Conversion (%)	Selectivity of IP (%)	Selectivity of MO (%)
HTox	15.8	53.0	15.5
Cr/HTox	25.2	73.9	11.9
Zr/HTox	36.8	72.5	8.9

^a : Experimental conditions: 0.6 g cat., acetone: 0.02 mL/min, 513 K and atmospheric pressure.

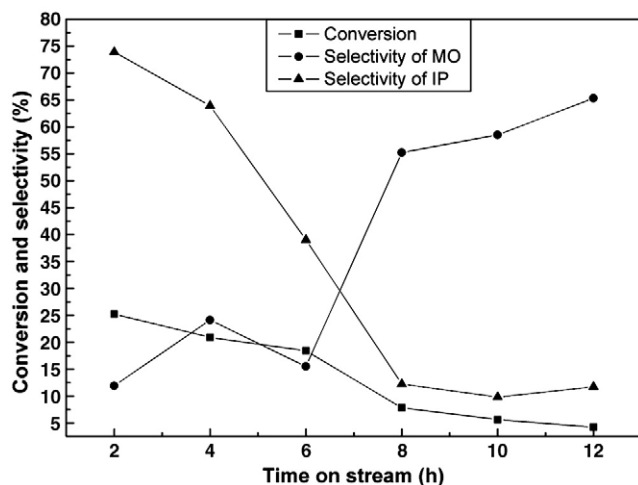


Fig. 4. Time-on-stream behavior for synthesis of IP over Cr/HTox.

heavier polymers bound to the catalyst surface [21]. We try to recycle the deactivated catalyst by calcination. After calcining at 773 K for 30 min, the reused catalyst did not recover the total activity (about 80% of the initial conversion.), which may be caused by the destroyed basic site by the water in the product.

4. Conclusions

Cr and Zr were successfully introduced into the lattice of the hydrotalcites via coprecipitation method and produced more irregular hydrotalcite structures. From the result of CO₂-TPD, the incorporation of Cr, Zr lead to creation of new strong basic sites and increase of the basic sites. The basicity of the mixed oxide was an important factor that influence the catalytic activity in the synthesis of IP. Consequently, the modified mixed oxide exhibited improved catalytic performances in the

synthesis of IP. Since the selectivity of IP reached 70% above, these doped mixed oxides should be potentially used in the synthesis of IP. Further improvement may be achieved by adjusting the Cr or Zr modification, as well as method of preparing the HT precursor.

Acknowledgements

The authors thank Professor Yongxiang Zhao and Xu Liang of Shanxi University for their helps on CO₂-TPD experiments and helpful discussions on the results.

References

- [1] F. Winter, X. Xia, B.P.C. Hereijgers, J.H. Bitter, A.J. van Dillen, M. Muhler, K.P. de Jong, *J. Phys. Chem. B* 110 (2006) 9211–9218.
- [2] J.C.A.A. Roelofs, D.J. Lensveld, A.J. van Dillen, K.P. de Jong, *J. Catal.* 203 (2001) 184–191.
- [3] D. Tichit, D. Lutić, B. Coq, R. Durand, R. Teissier, *J. Catal.* 219 (2003) 167–175.
- [4] O. Cairon, E. Dumitriu, C. Guimon, *J. Phys. Chem. C* 111 (2007) 8015–8023.
- [5] J. Barrault, A. Derouault, G. Courtois, J.M. Maissant, J.C. Dupin, C. Guimon, H. Martinez, E. Dumitriu, *Appl. Catal. A* 262 (2004) 43–51.
- [6] Z.P. Xu, H.C. Zeng, *Chem. Mater.* 12 (2000) 2597–2603.
- [7] J.I.D. Cosimo, V.K. Díez, C.R. Apesteguía, *Appl. Catal. A* 137 (1996) 149–166.
- [8] A.S. Canning, S.D. Jackson, E. McLeod, E.M. Vass, *Appl. Catal. A* 289 (2005) 59–65.
- [9] H. Hattori, *Appl. Catal. A* 222 (2001) 247–259.
- [10] A.A. Schutz, *USP* (1990) 4970191.
- [11] M. Ishino, M. Fukao, K. Sasaki, G. Suzukamo, M. Sasaki, *USP* (1993) 5243081.
- [12] R. Teissier, J. Kervennal, *USP* (1998) 5849957.
- [13] F.Z. Wang, K. Yang, Y.M. Chai, P.C. Gao, *Chin. J. Inorg. Chem.* 24 (2008) 1417–1423.
- [14] S. Velu, D.P. Sabde, N. Shah, S. Sivasanker, *Chem. Mater.* 10 (1998) 3451–3458.
- [15] J. Perez-Ramirez, S. Abello, N.M. van der Pers, *J. Phys. Chem. C* 111 (2007) 3642–3650.
- [16] S. Abelló, F. Medina, D. Tichit, J. Pérez-Ramírez, X. Rodríguez, J.E. Sueiras, P. Salagre, Y. Cesteros, *Appl. Catal. A* 281 (2005) 191–198.
- [17] P. Kustrowski, D. Sulkowska, L. Chmielarz, A. Rafalska-Lasocha, B. Dudek, R. Dziembaj, *Microporous Mesoporous Mater.* 78 (2005) 11–22.
- [18] J.I. Di Cosimo, V.K. Díez, M. Xu, E. Iglesia, C.R. Apesteguía, *J. Catal.* 178 (1998) 499–510.
- [19] M. Zamora, T. López, R. Gómez, M. Asomoza, R. Meléndrez, *Appl. Surf. Sci.* 252 (2005) 828–832.
- [20] J.I. Di Cosimo, V.K. Díez, C.R. Apesteguía, *Appl. Clay Sci.* 13 (1998) 433–449.
- [21] J.I. Di Cosimo, C.R. Apesteguía, *J. Mol. Catal. A* 130 (1998) 177–185.